J. Ind. Geophys. Union (May 2016)
v.20, no.3, pp: 309-315

Estimation of gas hydrate saturation using model based acoustic impedance inversion from Mahanadi offshore basin

Uma Shankar*[1], Debjani Bhowmick[2] and Kalachand Sain[3]
[1]Department of Geophysics, Institute of Science, Banaras Hindu University, Varanasi-221005
[2]CMPDI (HQ), Kanke Road, Rachi-834008
[3]CSIR-National Geophysical Research Institute, Uppal Road, Hyderabad – 500007
*Corresponding Author : umashankar_ngri@yahoo.com

ABSTRACT
The bottom simulating reflector (BSR), observed on seismic section in the Mahanadi offshore basin indicates the presence of gas hydrates. Gas hydrate saturation is estimated from electrical resistivity log based on Archie's empirical relation and/or from sonic velocity log using rock physics modeling approach at the vertical log position. The lateral and vertical extent of gas hydrates saturation over a larger area is obtained by post-stack impedance inversion of seismic data constrained by well log data. The inverted velocity coupled with rock physics modeling provides the estimation of gas hydrate saturation. The present study suggests that average gas hydrate saturation along a seismic line passing through site NGHP-01-19 in the Mahanadi Basin is about 3%. Gas hydrate saturation directly measured from the pressure cores, is found to be 2.4% at site NGHP-01-19, showing close correspondence with the estimation.

Key words: Gas hydrate, Acoustic velocity, Acoustic impedance inversion, Gas hydrate saturation.

INTRODUCTION

The Mahanadi (MN) Basin is a major sedimentary Basin of the east coast of India Figure 1. The MN Basin is characterized by thick accumulation (8-10 km) of sediments (Collett et al., 2008). Sediment input to the Bay of Bengal is dominated by the Ganges-Brahmaputra river system, which drains much of the Himalayas. The resulting sediment influx has built the Bengal Fan, the world's largest sediment accumulation. The sediment reaches to a maximum thickness of over 22 km on the Bangladesh shelf (Curray and Munasinghe, 1991). Various seismic indicators of the occurrences of gas hydrates were identified on multichannel seismic (MCS) data in the central and deeper parts of the MN Basin (Collett et al., 2008, Prakash et al., 2010, Sain and Gupta, 2012, Shankar and Riedel, 2014). These include bottom-simulating reflectors (BSRs), enhanced reflections below the BSR, channelized (cut-and-fill) deposition and seismic chimneys, faults, slumps/slides and sedimentary ridges (Bastia, 2006). The BSR occurs from about 200 to less than 300 meter below seafloor (mbsf) on MCS data in the central part of the basin (Shankar and Riedel, 2014). However, strong BSR could not be identified at some profiles, the top of the high-reflectivity band is interpreted to represent the base of the gas hydrate stability zone (BGHSZ) with free gas accumulations below, causing very high reflectivity (Collett et al., 2008; Shankar and Riedel, 2014). The overall sediment flux that is received in the MN Basin is mainly from the Mahanadi, Brahmani, Baitarani and Dhamara rivers system with a sediment load to the basin on the order of 7.1×10^{9} kg/yr (Subramanian, 1978) and total organic carbon (TOC) to be more than 1.5% (Collett et al., 2008; Sain and Gupta, 2012), which favors the formation of gas hydrates in this region. The MN Basin is also characterized by bathymetry, sediment thickness and geothermal gradient ranging from 40-55 °C/km (Sain et al., 2011).

The MN Basin was studied using high resolution MCS data (Bastia, 2006; Bastia et al., 2010a, b; Prakash et al., 2010; Shankar and Riedel, 2014) for the investigation of hydrocarbon prospect and gas hydrate occurrences. The area was also investigated using deep drilling by the Directorate General of Hydrocarbon (DGH) under the Indian National Gas Hydrate Program (NGHP) Expedition-01 (Collett et al., 2008).The NGHP Expedition-01 was completed successfully in the continental margins of India in April to June 2006 and gas hydrate samples were recovered by drilling and coring from sites NGHP-01-08, 09, 18 and 19 in the MN Basin. The in situ temperature measured at site NGHP-01-19 in the MN Basin shows the geothermal gradient of 52 °C/km (Collett et al., 2008) and the BSR depth of 205 mbsf (Collett et al., 2008; Shankar and Riedel, 2014). The 2D high resolution MCS data, which is used here reveals flat BSR that coincides with the BGHSZ followed by very high reflectivity (Collett et al., 2008; Shankar and Riedel, 2014). The interpreted BGHSZ is in good correspondence with the geothermal modeling of BGHSZ performed by Shankar and Riedel (2014).

Seismic data provides important information about the general geology of the area. However, extraction of physical properties information such as velocity, porosity, density etc. is a great challenge. The seismic inversion is a powerful tool for estimating detailed characteristics of the reservoir (Kumar et al., 2016). Different seismic inversion

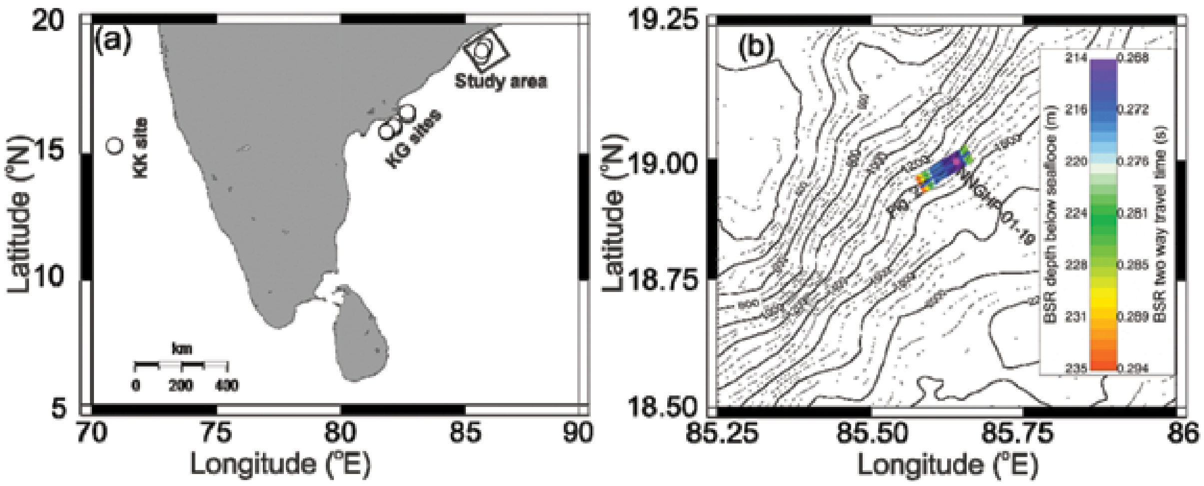

Figure 1. (**a**) Study area map in the Mahanadi Basin shown in box. (**b**) Bathymetry map of the Mahanadi Basin targeted during the drilling and coring of Indian National Gas Hydrate Drilling Expedition-01. Drilling sites are shown with black dots. The location of 2-D MCS line is shown with bold blue line passing through NGHP-01-19 site. The BSR depth below seafloor in meters and two way travel time below seafloor in seconds are also shown.

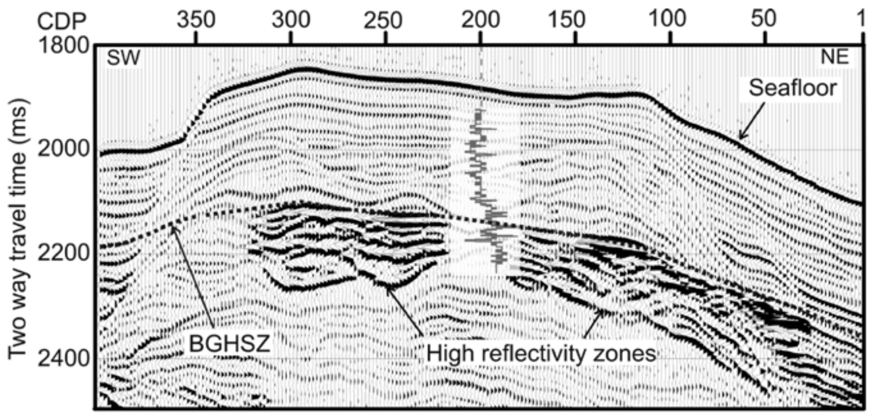

Figure 2. Sonic P-wave velocity log is overlain on seismic section crossing the Site NGHP-01-19, which was drilled in a gap between two similar channelized free-gas accumulations in order to safely obtain core and down hole log data from both above and below the expected BGHSZ (Collett et al., 2008). Top of the high reflectivity zone interpreted as BGHSZ. Dotted blue line represents the modeled BGHSZ (Shankar and Riedel, 2014).

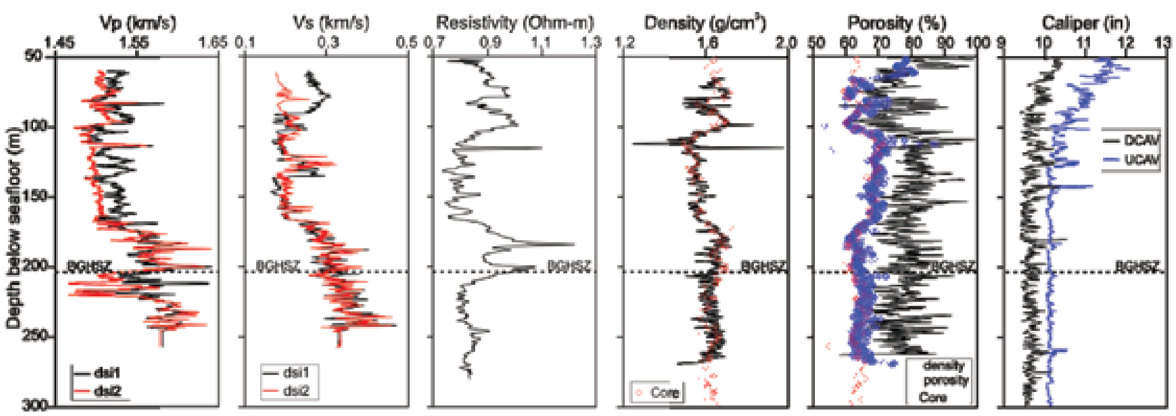

Figure 3. Suite of logs from site NGHP-01-19, including the sonic P and S-wave velocity, electrical resistivity, bulk density (RHOB), neutron porosity and caliper (DCAV, UCAV). Open red squares show density, porosity values measured from core samples and open blue squares are porosity derived from density log superimposed on the corresponding log curve. The BGHSZ is highlighted by the dotted black line.

methods are used commercially to derive detailed reservoir properties such as the lithology and fluid properties in combination with well log data and prior knowledge of geology (Riedel and Shankar, 2012). Model based acoustic impedance inversion was applied on stacked seismic data constrained by log data to derive physical properties of gas hydrate bearing sediments (Lu and McMechan, 2002; Dai et al., 2008; Wang et al., 2006; Riedel and Shankar, 2012; Shankar, 2016). To appraise the areal extent of gas hydrate in the MN Basin, gas hydrate saturation is estimated from physical properties derived from the acoustic impedance inversion coupled with rock physics modeling.

Seismic and log data

The high resolution 2-D seismic stacked data was made available to the NGHP from the Reliance Industries Limited for scientific research (Collett et al., 2008). The seismic data was also previously used for defining geophysical drilling targets and site selection for the NGHP Expedition-01. The BSR and BSR-like features have been identified on seismic data (Shankar and Riedel, 2014), and Figure 2 shows a SW-NE oriented section crossing the site NGHP-01-19, which was drilled at ~1422 m water depth (Collett et al., 2008). The BSR was estimated at a depth of 205 mbsf (0.125 s TWT) using a constant velocity of 1610 m/s for the entire sediment column above the BGHSZ (Collett et al., 2008). The site NGHP-01-19 was drilled up to depth of only 300 mbsf between two anomalous high reflective zones. Presence of bright reflectivity zones beneath the BGHSZ indicates likely presence of free gas zones Figure 2.

Four sites were drilled in the MN Basin, and extensive Logging-While-Drilling (LWD)/Measurement-While-Drilling (MWD) data were acquired at site NGHP-01-08 and 09 without coring. The Site NGHP-01-18 was only cored and wire-line logged, and suits of logs were acquired at Site NGHP-01-19 to measure the physical properties of gas hydrate-bearing sediments. Site NGHP-01-19 was continuously cored up to 305 mbsf (Collett et al., 2008). At site NGHP-01-19, the gas hydrate is unevenly distributed in very thin layers and lies just above interpreted BGHSZ (Collett et al., 2008). Gas hydrate was found at 177-204 mbsf and maximum gas hydrate saturation was found to be 2.4% of pore space at a depth 193.5 mbsf at site NGHP-01-19A by pressure core measurement. Gas hydrate found at depth interval of 177-204 mbsf with maximum gas hydrate saturation of 10%. Hydrate saturation percentage was estimated from electrical resistivity log and pore-water chlorinity data (Collett et al., 2008; Shankar and Riedel, 2014).

Figure 3 shows the suite of logs at site NGHP-01-19. Wire-line logging with the dipole sonic imager (DSI) tools was utilized to measure the P- and S-wave velocities. Two run of DSI tools (DSI1 and DSI2) are shown in Figure 3 with different colors. The sonic velocity log shows an increasing trend of P- and S-wave velocities with depth, and the maximum velocity is observed just above the BSR at ~205 mbsf Figure 3. A sudden drop in P-wave velocity to ~1.53 km/s is observed just below the BGHSZ and the velocity again increases up to 1.63 km/s Figure 3. Resistivity log consistent with the P-wave velocity log trend and relatively high resistivity zone maximum up to ~1.2 ohm-m (165-185 m) is observed. But no visible gas hydrate samples were recovered from the site NGHP-01-19. However, the IR camera has identified a steady decrease in temperature with depth measured on the core liner above 205 mbsf. This is interpreted as the indication of gas hydrate disseminated in the formation above BGHSZ (Collett et al., 2008, Shankar and Riedel, 2014). Density and porosity measurements of core samples are superimposed on the corresponding logs. Density log matches reasonably well with the measured core despite the irregular hole size. The porosity calculated from density log shows good correspondence with the porosity measured from the core samples, indicating a precise measurement of density log data Figure 3. The neutron porosity log showing consistently higher than the measured core porosity is because of the influence of mineral-bound water in these clay dominated sediments (Collett et al., 2008) Figure 3. The shallow zone of the log above 60 mbsf cannot be used, as the caliper log shows a much enlarged hole near the seafloor.

Material and methods

Acoustic impedance provides rock properties information and has been used to describe rock types. Rock properties information has also been used as direct hydrocarbon indicator (Latimer et al., 2000). Model based acoustic impedance inversion can be used to derive acoustic impedance variation based on seismic data and low frequency impedance information obtained from well logs (Lindseth, 1979). In this study we performed post-stack impedance inversion along a seismic section in the MN Basin. The model based acoustic impedance inversion is based on perturbation of a low frequency P-impedance model until the synthetic traces matches the observed seismic data. This method is based on the convolution of a seismic wavelet with the earth's reflectivity (Lu and Mcmechan, 2002) as:

$$S_t = [W_t * R_t] \quad \text{..........(i)}$$

where S_t is the seismic trace, W_t is the seismic wavelet and R_t is the reflectivity.

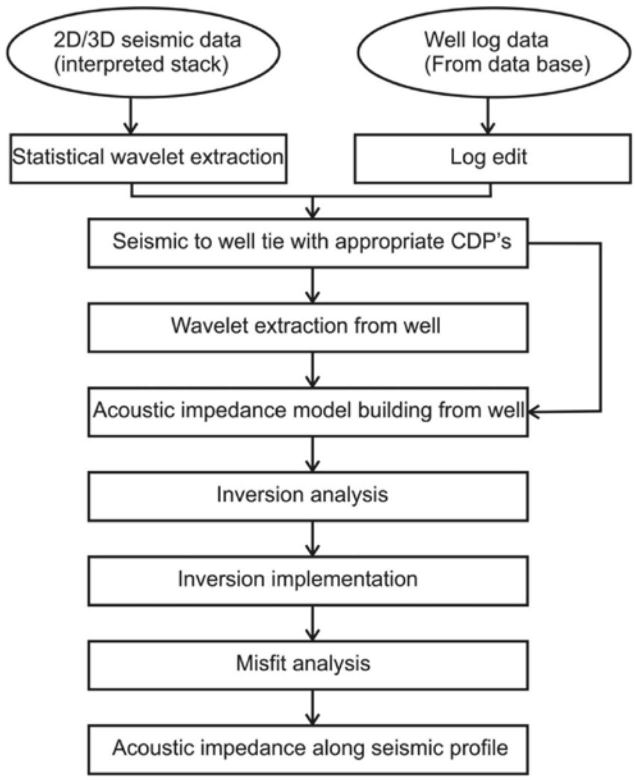

Figure 4. Post stack model-based acoustic impedance inversion simplified flow chart.

The zero-offset P-wave reflectivity R_t, is related to the acoustic impedance Z of the earth as:

$$R_t = \frac{Z_{t+1} - Z_t}{Z_{t+1} + Z_t} \qquad \text{..........(ii)}$$

where $Z_t = \rho v_t$ is the impedance of the t^{th} layer (ρ is density and v_t is P-wave velocity of the t^{th} layer), and Z_{t+1} is the impedance of the underlying layer. We can invert equation (ii) for the P-impedance by recursive method.

$$Z_{t+i} = Z_t \left[\frac{1+R_t}{1-R_t} \right] \qquad \text{..........(iii)}$$

From equation (iii) we can effectively transform reflection seismic traces to P-impedance. However, all inversion algorithms suffer from the non-uniqueness problem. This means that there is more than one possible geological model, consistent with the seismic data. In practice, this problem is handled by using geological constraints, provided by well logs. Gas hydrate saturation can be estimated from acoustic impedance of seismic data computed using different post-stack impedance inversion techniques such as: model-based, sparse spike and band limited inversion (Lu and Mcmechan, 2002; Dai et al., 2008; Riedel and Shankar, 2012; Shankar, 2016). Model -based post- stack inversion is used (Russell and Hampson, 1991) for computation of acoustic impedance from seismic data. Figure 4 shows the detail flow chart of the model based acoustic impedance analysis and inversion. In this study an effective medium model on inverted P-wave velocity is applied to obtain gas hydrate saturations. The modeled P-wave velocities of gas hydrate bearing sediments assumes the pore-filling form of gas hydrate, as it affects only the P-wave velocity (Singha et al., 2014).

Following the analysis at well location, the model based inversion was performed using the extracted wavelet from the seismic stacked data and a low frequency initial model with prior geological information such as the reservoir geometry. This can be done by interpretation of geological features on seismic section. In this study, two horizons were interpreted on the basis of prominent amplitudes and characteristics such as the sea floor and BSR. A low frequency initial acoustic impedance model was computed from the P-wave impedance log at well position and extrapolated along the seismic line. Figure 5a shows the acoustic impedance initial model along the seismic line. The P-wave impedance along the line interpolated from the well NGHP-01-19 shows increasing impedance with depth. Simultaneously, the inverted P-wave velocity obtained at the well location and extrapolated along the seismic line crossing the well NGHP-01-19 is shown in Figure 5b.

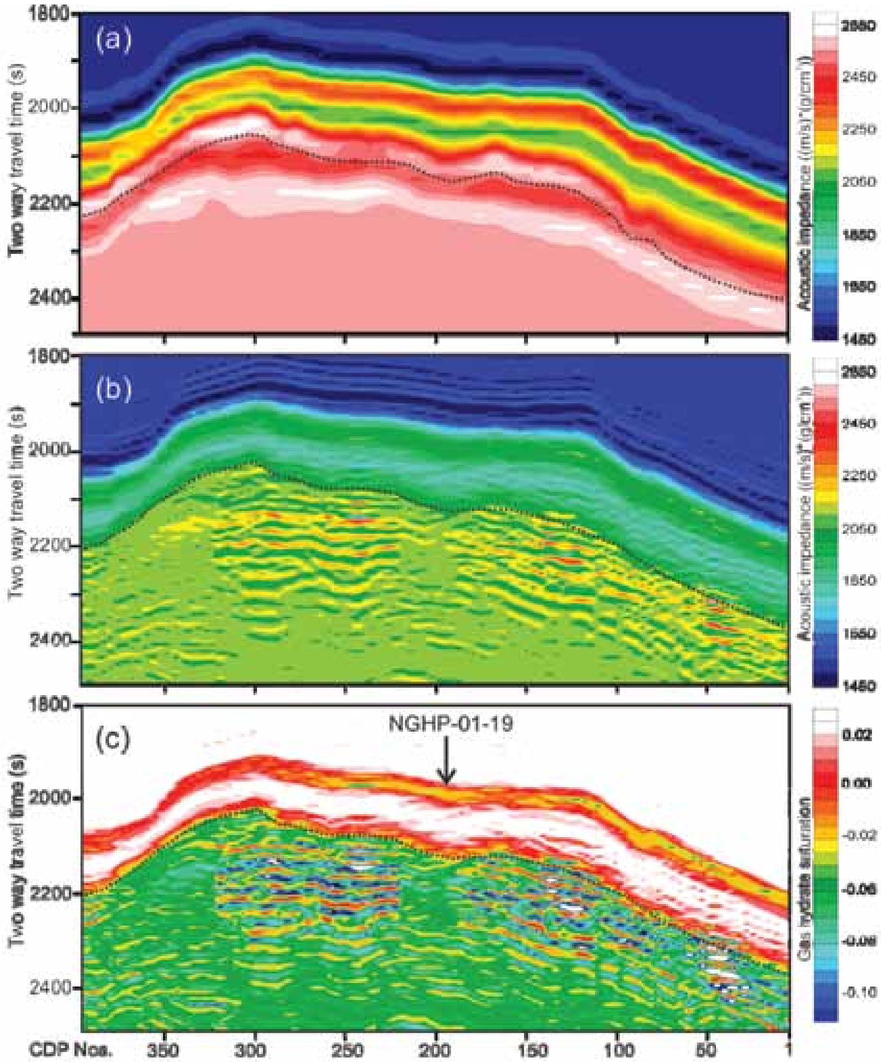

Figure 5. (**a**) Initial model for model based acoustic impedance inversion of 2D multi-channel seismic data, (**b**) Result from model based P-impedance inversion of the stacked volume along 2D seismic profile crossing well NGHP-01-19. Color-code shows inverted P- impedance in ((m/s) × (g/cc)), (**c**) Estimated gas hydrate saturation along 2D seismic profile using effective medium rock physics model on inverted velocity. The well location is marked with arrow. Black dotted curve shows the BGHSZ.

RESULTS AND DISCUSSION

The acoustic impedance is calculated by model-based inversion constrained by well logs data at site NGHP-01-19 passing through the seismic line. The inversion of the hydrates region uses the interpreted information from seafloor, BSR and key reflectors to build structural model and to control the low frequency part of the model. To calculate impedance, the density and velocity logs were used along with low frequency (15 Hz) initial model.

Well-to-seismic correlation provides an efficient way to establish hydrate events on seismic data and for the calibration of gas hydrate estimation using an appropriate model. A well-based, zero-offset synthetic seismogram is created and compared with the post-stack seismic traces at the well location. The first step of seismic inversion is to correlate the well with the seismic stacked data, in which events recorded on the well log are correlated with the events recorded on the seismic data. To start a well to seismic tie, synthetic traces are generated to correlate with the recorded seismic traces. A suitable wavelet is extracted from the observed seismic data. The post-stack impedance inversion analysis is performed at the well location NGHP-01-19 to evaluate the accuracy of the inversion and to calculate an amplitude scaling factor between the seismic data and the impedance at the well site. The P-impedance inverted from single trace at the well location, and then a synthetic trace generated using this impedance and the extracted P-wavelet is compared with the extracted trace from the seismic data at well location.

To estimate gas hydrate saturation along the seismic line, physical parameters required are velocity, porosity and density. Density estimated simply by dividing inverted impedance by inverted velocity. Porosity estimated from the derived density along the seismic line from density porosity relationship $\phi = (\rho_g - \rho_b)/(\rho_g - \rho_w)$. Where ρ_b is the formation bulk density of the medium, ρ_w is the density of pore water which is 1030 kg/m^3 and ρ_g is the average grain density equal to 2750 kg/m^3 measured in the core moisture and density analysis. The porosity estimation using this method is tested at well log site NGHP-01-19. The inverted P-wave velocity was then translated into the saturation of gas hydrate by invoking the effective medium rock physics theory to the time/depth varying porosity-profile and assumed mineralogical mix (Shankar and Riedel, 2011; Shankar and Riedel, 2013; Shankar et al., 2013). The saturation of gas hydrate estimated along the SW-NE trending seismic profile shows as high as 3.0% of the pore space Figure 5c.

CONCLUSIONS

The impedance was calculated from the stacked seismic data using a post-stack model-based acoustic impedance inversion method. The gas hydrate saturation derived from the model-based acoustic impedance coupled with rock physics modelling, varies up to 3.0% of the pore space along the seismic line. The gas hydrate saturation (2.4% of the pore) directly measured from the recovered core shows close correspondence with the estimated values at drilling site NGHP-01-19. Estimation of this kind of saturation of gas hydrates provides a quick idea of the areal extent of gas hydrate along a seismic line.

ACKNOWLEDGEMENTS

We thank the gas hydrate science team of National Gas Hydrate Expedition 01 (NGHP-01) and crew members. The Director of CSIR-National Geophysical Research Institute (NGRI), Hyderabad is thanked for encouragement and support. In addition, U Shankar is grateful to the Indo-US Science and Technology Forum (IUSSTF), Govt. of India, New Delhi for the Indo-US Fellowship-2013. This is a contribution to the SHORE Project under the 12th Five Year Plan of CSIR-NGRI.

Compliance with Ethical Standards

The authors declare that they have no conflict of interest and adhere to copyright norms.

REFERENCES

Bastia, R., 2006. An overview of Indian sedimentary basins with special focus on emerging east coast deepwater frontiers. The Leading Edge, v.25, no.7, pp: 818–829.

Bastia, R., Radhakrishna, M., Srinivas, T., Nayak, S., Nathaniel, D.M., and Biswal, T.K., 2010a. Structural and tectonic interpretation of geophysical data along the Eastern Continental Margin of India with special reference to the deepwater petroliferous basins. Journal of Asian Earth Sciences, v.39, pp: 608–619.

Bastia, R., Radhakrishna, M., Das, S., Kale, A.S., and Catuneanu, O., 2010b. Delineation of the 85ºE ridge and its structure in the Mahanadi Offshore Basin, Eastern Continental Margin of India (ECMI), from seismic reflection imaging. Marine and Petroleum Geology, v.27, no.9, pp: 1841–1848.

Curray, J.R., and Munasinghe, T., 1991. Origin of the Rajmahal Traps and the 85ºE Ridge: preliminary reconstructions of the trace of the Crozet hotspot. Geology., v.19, no.12, pp: 1237–1240.

Collett, T.S., Riedel, M., Cochran, J.R., Boswell, R., Presley, J., Kumar, P., Sathe, A.V., Sethi, A., Lall, M., Sibal, V. and NGHP Expedition 01 Scientists, 2008.National Gas Hydrate Program Expedition 01 initial reports. Directorate General of Hydrocarbons, New Delhi.

Dai, J., Snyder, F., Gillespie, D., Koesoemadinata, A., and Dutta, N., 2008. Exploration for gas hydrates in the deepwater, northern Gulf of Mexico: Part I, A seismic approach based on geologic model, inversion, and rock physics principles. Marine and Petroleum Geology, v.25, no.9, pp: 830–844.

Kumar, R., Das, B., Chatterjee, R., and Sain, K., 2016. A Methodology of Porosity Estimation from Inversion of Post-Stack Seismic Data. Journal of Natural Gas Science and Engineering, v.28, pp: 356–364.

Latimer, R.B., Davison, R., and Riel, P.V., 2000. An interpreter's guide to understanding and working with seismic-derived acoustic impedance data. The Leading Edge, v.19, no.3, pp: 242–256.

Lindseth, R.O., 1979. Synthetic sonic logs – A process for stratigraphic interpretation. Geophysics, v.44, no.1, pp: 3–26.

Lu, S., and McMechan, G.A., 2002. Estimation of gas hydrate and free gas saturation, concentration, and distribution from seismic data. Geophysics, v.67, no.2, pp: 582–593.

Prakash, A., Samanta, B. G., and Singh, N.P., 2010. A seismic study to investigate the prospect of gas hydrate in Mahanadi deep water basin, northeastern continental margin of India. Marine Geophysical Researches, v.31, no.4, pp: 253–262.

Russell, B., and Hampson, D., 1991. Comparisons of post stack inversion methods: 61stAnnual International Meeting, SEG, Expanded Abstracts v.10, pp: 876–878.

Riedel, M., and Shankar, U., 2012. Combining acoustic impedance and seismic similarity for robust gas hydrate concentration estimate – A case study from Krishna Godavari Basin, East coast of India. Marine and Petroleum Geology, v.36, no.1, pp: 35–49.

Sain, K., Rajesh, V., Satyavani, N., Subbarao, K.V., and C. Subrahmanyan. 2011. Gas hydrates stability thickness map along the Indian continental margin. Marine and Petroleum Geology, v.28, no.10, pp: 1779–1786.

Sain K., and Gupta, H.K., 2012. Gas hydrates in India: Potential and Development. Gondwana Research, v.22, no.2, pp: 645–657.

Singha, D.K., Chatterjee, R., Sen, M.K., and Sain, K., 2014. Pore pressure prediction in gas-hydrate bearing sediments of Krishna-Godavari basin, India. Marine Geology., v.357, pp: 1–11.

Subramanian, V., 1978. Input by Indian rivers into the world oceans. Proc. Indian Acad. Sci. Sect. A: Earth Planetary Science, v.87, no.7, pp: 77–88.

Shankar, U., and Riedel, M., 2011. Gas hydrate saturation in the Krishna-Godavari basin from P-wave velocity and electrical resistivity logs. Marine and Petroleum Geology, v.28, no.10, pp: 1768–1778.

Shankar, U., and Riedel, M., 2013. Heat flow and gas hydrate saturation estimates from Andaman Sea, India. Marine and Petroleum Geology, v.43, pp: 434–449.

Shankar, U., Gupta D.K., Bhowmick, D., and Sain, K., 2013. Gas hydrate and free gas saturations using rock physics modeling at site NGHP-01-05 and 07 in the Krishna Godavari Basin, Eastern Indian Margin. Journal of Petroleum Science and Engineering, v.106, pp: 62–70.

Shankar, U., and Riedel, M., 2014. Assessment of gas hydrate saturation in marine sediments from resistivity and P-wave velocity log measurements in the Mahanadi basin, India. Marine and Petroleum Geology, v.58, part A, pp: 265–277.

Shankar, U., 2016. Gas hydrate saturation from seismic data constrained by log data in the Krishna-Godavari Basin. Journal of Petroleum Exploration and Production Technology., DOI 10.1007/s13202-015-0170-1., v.6, no.1, pp: 13–23.

Wang, X., Wu, S., Xu, N., and Zhang, G., 2006. Estimation of gas hydrate saturation using constrained sparse spike inversion: Case study from the Northern South China Sea. Terrestrial of Atmospheric Oceanic Science, v.17, no.4, pp: 799–813.